Investigating Habenula Functional Connectivity and Reward-Related Activity in Obesity Using Human Connectome Project Data

Slomp, M.; de Lange, I.G.S.; Mul, J.D.; Schrantee, A.; la Fleur, S.E.

DOI
10.1089/brain.2023.0034

Publication date
2023

Document Version
Final published version

Published in
Brain Connectivity

BRAIN CONNECTIVITY
Volume 13, Number 9, 2023

DOI: 10.1089/brain.2023.0034

Investigating Habenula Functional Connectivity and Reward-Related Activity in Obesity Using Human Connectome Project Data

Margo Slomp,[1–4] Ilke G.S. de Lange,[1,4] Joram D. Mul,[2,5] Anouk Schrantee,[2,6,*] and Susanne E. la Fleur[1–4,*]

Abstract

Introduction: The habenula, a brain region involved in aversion, might negatively modulate caloric intake. Functional magnetic resonance imaging (fMRI) studies reported associations between weight loss and habenula functional connectivity. However, whether habenula resting-state functional connectivity (rsFC) and reward-related activity are altered in obesity is yet unknown.
Methods: Using data from the Human Connectome Project, we included 300 subjects with various body mass indexes (BMIs) and a healthy long-term blood glucose (hemoglobin A1c [HbA1c]). In addition, we investigated a potential BMI × HbA1c interaction in a separate cohort including subjects with prediabetes ($n = 72$). Habenula rsFC was assessed using a region of interest (ROI)-to-ROI analysis. Furthermore, a separate analysis using gambling task fMRI data focused on reward-related habenula activity.
Results: We did not find an association between BMI and habenula rsFC for any of the ROIs. For the exploratory analysis of the BMI × HbA1c effect, a significant interaction effect was found for the habenula–ventral tegmental area (VTA) connection, but this did not survive multiple comparisons correction. Monetary punishment compared with reward activated the bilateral habenula in the BMI sample, but this activity was not associated with BMI.
Discussion: In conclusion, we did not find evidence for an association between BMI and habenula rsFC or reward-related activity. However, there might be an interaction between BMI and HbA1c for the habenula-VTA rsFC, suggestive of a role of the habenula in glucose regulation. Future studies should focus on metabolic parameters in their experimental design to confirm our findings and explore the precise role of the habenula in metabolism.

Impact Statement

While obesity and its comorbidities are a major health concern, little attention has been given to potential negative regulators of caloric consumption, such as the habenula. Using the high-quality, publicly available, Human Connectome Project data set, a sufficient sample size for detecting resting-state functional connectivity (rsFC)

[1]Endocrine Laboratory, Department of Laboratory Medicine, Amsterdam UMC, Location University of Amsterdam, Amsterdam, The Netherlands.
[2]Amsterdam Neuroscience, Amsterdam, The Netherlands.
[3]Amsterdam Gastroenterology Endocrinology & Metabolism, Amsterdam, The Netherlands.
[4]Metabolism and Reward Group, Royal Netherlands Academy of Arts and Sciences, Netherlands Institute of Neuroscience, Amsterdam, The Netherlands.
[5]Brain Plasticity Group, Swammerdam Institute for Life Sciences, Faculty of Science, University of Amsterdam, Amsterdam, The Netherlands.
[6]Department of Radiology and Nuclear Medicine, Amsterdam UMC, University of Amsterdam, Amsterdam, The Netherlands.
*These two authors contributed equally to this work.

differences was obtained. We did not find associations between habenula rsFC and obesity in individuals with a healthy blood glucose. Our data do suggest, however, that metabolic parameters are important to include in future research. More tailored approaches are crucial to investigate a possible role of the habenula in negatively regulating caloric consumption and its potential therapeutic role.

Keywords: blood glucose; functional magnetic resonance imaging; habenula; Human Connectome Project; monetary punishment; obesity

Introduction

Obesity, defined as a body mass index (BMI) above 30, affects more than 600 million adults worldwide (Afshin et al., 2017) and is linked to several comorbidities, including metabolic and cardiovascular disorders (Martin-Rodriguez et al., 2015). Readily available, affordable, and convenient foods that are high in calories and very palatable are thought to be an important contributing factor (Stice et al., 2013). The brain receives central and peripheral information about the energy status and integrates this information. Brain regions, such as the hindbrain and hypothalamus, then initiate or terminate consummatory behavior to meet energy demand (Waterson and Horvath, 2015). In addition, brain regions, such as the nucleus accumbens (NAc), ventral tegmental area (VTA), and amygdala, are involved in the motivation for reward-seeking behavior and the reinforcing value of food, which can stimulate consummatory behavior beyond homeostatic needs (Berridge, 2009; Berthoud, 2011; Berthoud and Morrison, 2008).

Thus, the brain plays a crucial role in regulating feeding behavior, and previous magnetic resonance imaging (MRI) studies have revealed that obesity affects brain morphology and function. For example, obesity is associated with decreased total gray matter volume, as well as region-specific reductions in reward-related brain areas (Gunstad et al., 2008; Herrmann et al., 2019). In terms of functional changes, functional magnetic resonance imaging (fMRI) studies showed that obesity is associated with altered resting-state functional connectivity (rsFC) in various networks, including increased connectivity between reward-related areas (Doucet et al., 2017; Kullmann et al., 2012; Stoeckel et al., 2009).

In response to food cues, increased activity was observed in reward-related areas, including pregenual anterior cingulate cortex (pgACC) and insula, driving overconsumption (Avery et al., 2017; García-García et al., 2013; Li et al., 2020; Scharmüller et al., 2012; Stice et al., 2008; Wang et al., 2020). Whereas many studies focused on reward-related overeating, to battle obesity, it is important to also understand the role of areas with a negative impact on consummatory behavior.

A potential negative regulator of consummatory behavior is the habenula, a small epithalamic nucleus, which is activated upon punishment signaling negative motivational value (Lawson et al., 2014; Matsumoto and Hikosaka, 2007). It receives input from many brain regions, including homeostatic information from the hypothalamus, and projects to the VTA and dorsal raphe nucleus to modulate dopamine and serotonin signaling, respectively (Ji and Shepard, 2007; Omelchenko et al., 2009; Yang et al., 2008). Rodent studies showed that inhibition of the projection from the hypothalamus to the habenula in mice increases consumption of palatable foods (Stamatakis et al., 2016). In contrast, lesioning the habenula in rats improved glucose metabolism and contributed to better metabolic health (Qu et al., 2020).

Human fMRI studies that focus on the habenula have been sparse, possibly due to the challenges posed by the small size of the habenula. Nevertheless, recent studies have shed light on functional connectivity (FC) of the habenula in individuals with weight loss, caused by cancer or bariatric surgery. First, cancer-associated weight loss was associated with reduced FC between the habenula and hypothalamus and between the habenula and NAc (Maldonado et al., 2018). Second, weight loss after bariatric surgery was associated with changes in structural connectivity of the habenula with homeostatic and reward-related regions, as well as changes in local FC density within the habenula (Wang et al., 2023; Wang et al., 2022). However, to date, no human fMRI studies have yet investigated habenula FC in relation to obesity.

To address this, we studied the role of the habenula in obesity by investigating the relation between BMI and rsFC, and between BMI and habenula activation upon monetary punishment in a gambling task fMRI (tfMRI). We utilized high-resolution, 3T resting-state fMRI (rs-fMRI) data from the Human Connectome Project (HCP), a large-scale collaboration, with the goal to unravel human connectivity by collecting and sharing high-quality data (Van Essen et al., 2013). Using a region of interest (ROI)-to-ROI approach, we investigated whether habenula rsFC with reward-related areas (amygdala, insula, NAc, hypothalamus, pgACC, VTA) would correlate with BMI during resting state. Next, we investigated if monetary punishment in a gambling tfMRI would reveal increased activity of the habenula and if this habenula activity was positively associated with BMI. Finally, we performed an exploratory analysis in a secondary data set, including individuals with prediabetes (defined as hemoglobin A1c [HbA1c] ≥5.7%) to explore if we would observe an interaction effect between BMI and HbA1c on habenula rsFC and reward-related activity.

Methods

Subjects

Data were obtained from the WU-Minn HCP Consortium's 1200 Subjects Release (WU-Minn, 2017; Van Essen et al., 2013). This study included healthy participants ($n = 1203$) between 2012 and 2015, and written informed consent for a protocol approved by Washington University in St. Louis and University of Minnesota Institutional Review Boards was obtained from each individual before study procedures commenced. Details of inclusion and exclusion criteria are described in the study by Van Essen et al. (2013), but subjects were between 22 and 35 years of age and required to be broadly considered healthy to ensure an optimal representation of the general population. Subjects with illnesses such as cardiovascular disease or diabetes were

excluded due to the possible impact on neuroimaging data quality. We only included unrelated individuals with known BMI and HbA1c values.

To study the relation between habenula rsFC and tfMRI activity with BMI, all unrelated subjects with a BMI ≥30 and HbA1c <5.7% were selected ($n = 100$). HbA1c is a long-term measure of blood glucose, with values below 5.7% considered healthy and 5.7% and above considered to be prediabetic, which is a disturbance in metabolic health that might influence the FC (Sadler et al., 2021). For comparison, the same number of lean and overweight subjects was added (total $n = 300$) and pair-matched (using *optmatch* 0.9-7 package in R) on age, sex, ethnicity, socioeconomic status (SES), depression score, smoking status, handedness, and the number of available resting-state scans. SES was calculated as per Wani (2019); handedness was assessed using the Edinburgh Handedness questionnaire (Oldfield, 1971); and depression score was a subclinical measure taken from the NIH Toolbox Negative Affect Survey Sadness Subscale (Gershon et al., 2013). A BMI between 18.5 and 25 was considered lean, between 25 and 30 overweight, and above 30 was considered obese. Sample characteristics for the BMI sample are described in Table 1.

Given that obesity is associated with changes in glucose metabolism (Bonadonna and De Fronzo, 1991; Eckel et al., 2005; Jallut et al., 1990), the effects of BMI could be dependent on blood glucose levels; therefore, an additional exploratory analysis of the interacting effect of HbA1c and BMI on habenula FC was performed. For this exploratory analysis, we included subjects with an HbA1c value higher than 5.7% (the cutoff for prediabetes) and matched healthy HbA1c individuals on BMI, age, sex, ethnicity, SES, depression score, smoking status, and handedness. This led to the HbA1c sample, a set of 36 prediabetic subjects and 36 healthy controls ($n = 72$), all unrelated (Table 2).

Data collection and preprocessing

Details of HCP data collection have been described in detail previously (Uğurbil et al., 2013). The MRI data were collected using a 3T Connectome Skyra (Siemens, Erlangen, Germany) scanner with a 32-channel head coil on two consecutive days. Anatomical scans included two T1-weighted (T1w) magnetization-prepared rapid gradient-echo (MPRAGE) anatomical sequences with 0.7 mm isotropic resolution (TR = 2400 ms, TE = 2.14 ms) (Glasser et al., 2013). rs-fMRI data were collected as four 15-min gradient-echo echo planar imaging runs over 2 days (2.0 mm isotropic resolution, TR = 720 ms, TE = 33.1 ms, paired right-to-left/left-to-right (RL/LR) phase encoding, MB = 8). For the gambling tfMRI, two runs (LR/RL phase encoding) of 3:12 min were collected using the same parameters. Reward-related blood oxygen level-dependent (BOLD) signal was measured for monetary reward and punishment during a card-guessing gambling task (Barch et al., 2013; Forbes et al., 2009). In short, participants had to guess if a number (ranging from 1 to 9) on a card was higher or lower than 5 to win or lose money.

All fMRI data were preprocessed by HCP with the minimal preprocessing pipelines described previously, including spatial distorting correction, motion correction, spatial registration, and normalization to Montreal Neurological Institute (MNI) coordinates (Glasser et al., 2013).

Habenula and ROI identification

The habenula seeds were created per individual using a deep learning V-Net-based algorithm that uses the T1w anatomical scan as input (Kim and Xu, 2022). Due to the small size of the habenula, we checked the functional habenula seed size with the anatomical seed size per subject, as small changes can have significant effects on functional output, according to the study by Ely et al. (2016). To control for activity from neighboring thalamus nuclei and investigate the unique correlation of habenula activity, control seeds in the thalamus were created. To this end, the average bilateral habenula seed was moved in the anterior direction (dorsomedial nucleus of thalamus [DM]) and moved laterally (centromedial nucleus of thalamus [CM]), as per Ely et al. (2016).

Bilateral MNI ROIs of the NAc, amygdala, pgACC, and insula were retrieved from FMRIB Software Library (FSL) Harvard-Oxford Subcortical Structural Atlas, the MNI Structural Atlas, and the Schaefer Atlas (Collins et al., 1995; Desikan et al., 2006; Schaefer et al., 2018). For the VTA, an open-access atlas was used to create an ROI in MNI space (Pauli et al., 2018). Individual subject-specific segmentation of the hypothalamus ROI was performed using a publicly available deep convolution neural network algorithm, using resampled T1w scans as input (Billot et al., 2020). All seeds and ROIs are used probabilistic, except for the pgACC as this was only available binary, and are displayed in Figure 1.

rsFC analysis

In addition to the HCP minimal preprocessing pipelines, resting-state data were high-pass temporal filtered (cutoff = 2000 sec) and denoised using ICA-FIX (Smith et al., 2013) before it was made available to download. Subsequently, we used the CONN toolbox in MATLAB (R2016b, version 9.0.0.341460; Mathworks, Inc.) to perform additional preprocessing and first-level analyses (Whitfield-Gabrieli and Nieto-Castanon, 2012). Additional preprocessing included functional outlier detection based on Artifact Detection Tools (ART)-scrubbing, application of a band-pass (0.01–0.1 Hz) filter, confound regression of six rigid-body motion parameter and their temporal derivatives, and ''CompCor'' denoising of principal noise components associated with white matter and cerebrospinal fluid signals (Behzadi et al., 2007).

Frame-wise displacement (FD) was calculated after ART-scrubbing, as a measure of residual motion. The first-level ROI-to-ROI analysis consisted of a multivariate regression with the habenula, DM, and CM thalamic seeds as sources and NAc, VTA, amygdala, insula, pgACC, and hypothalamus as ROIs, resulting in the unique correlation of the habenula seed with the ROIs, while controlling for thalamic connectivity per individual. For each ROI, bilateral seeds and ROIs were used.

Gambling tfMRI analysis

Preprocessed parameter estimates (BOLD) for the punishment, reward, and punishment>reward contrasts were downloaded from HCP. After the minimal preprocessing pipelines, tfMRI data were spatially smoothed (FWHM = 4 mm) (Barch et al., 2013). Then, the 4D time series were used to estimate parameter estimates using a general linear model using FMRIB's improved linear model with

Table 1. Subject Characteristics for the Body Mass Index Sample, with a Healthy Hemoglobin A1c, and an Even Distribution of Body Mass Index Categories ($N = 300$)

	Lean (BMI >18.5), n = *100*	*Overweight (BMI 25–30),* n = *100*	*Obese (BMI >30),* n = *100*	*All subjects,* n = *300*	*Statistics*[a]	*Tukey's* post hoc
Age, years	28.42 ± 3.86	28.85 ± 3.44	28.96 ± 3.57	28.74 ± 3.63	$F(2,297) = 0.62$, $p = 0.54$	
Sex, F/M	51 F/49 M	42 F/58 M	50 F/50 M	143 F/157 M	$\chi(2) = 1.95$, $p = 0.38$	
Ethnicity	Am. Indian: 0 Asian: 2 Black: 8 More than one: 4 Unknown: 6 White: 86	Am. Indian: 0 Asian: 1 Black: 15 More than one: 1 Unknown: 1 White: 82	Am. Indian: 0 Asian: 1 Black: 16 More than one: 4 Unknown: 5 White: 74	Am. Indian: 0 Asian: 4 Black: 39 More than one: 9 Unknown: 6 White: 242	$\chi(8) = 13.35$, $p = 0.10$	
BMI, kg/m^2	22.60 ± 1.52	27.15 ± 1.44	33.43 ± 2.97	27.73 ± 4.91	$F(2,297) = 672$, $p < 0.01$***	Ov-Le: $p < 0.01$*** Ob-Le: $p < 0.01$*** Ob-Ov: $p < 0.01$***
SES	21.05 ± 5.66	20.69 ± 6.11	19.80 ± 6.49	20.52 ± 6.10	$F(2,297) = 1.11$, $p = 0.33$	
Systolic blood pressure, mmHg	119.70 ± 12.40	125.20 ± 12.77	129.50 ± 14.19	124.80 ± 13.70	$F(2,295) = 14.01$, $p < 0.01$**	Ov-Le: $p < 0.01$* Ob-Le: $p < 0.01$** Ob-Ov: $p = 0.06$
Diastolic blood pressure, mmHg	73.43 ± 8.95	77.81 ± 9.81	80.40 ± 11.32	77.19 ± 10.44	$F(2,295) = 12.14$, $p < 0.01$**	Ov-Le: $p < 0.01$** Ob-Le: $p < 0.01$** Ob-Ov: $p = 0.17$
HbA1c, %	5.16 ± 0.28	5.24 ± 0.25	5.26 ± 0.24	5.22 ± 0.26	$F(2,297) = 3.99$, $p = 0.02$*	Ov-Le: $p = 0.06$ Ob-Le: $p = 0.03$* Ob-Ov: $p = 0.93$
Handedness	70.3 ± 34.99	67.85 ± 41.55	64.6 ± 43.64	67.58 ± 40.16	$F(2,97) = 0.51$, $p = 0.60$	
Depression score	46.34 ± 8.97	45.56 ± 7.47	46.84 ± 7.87	46.25 ± 8.12	$F(2,297) = 0.63$, $p = 0.53$	
Smoking, yes/no	87 no/13 yes	82 no/18 yes	76 no/24 yes	245 no/55 yes	$\chi(2) = 4.05$, $p = 0.13$	
rs-fMRI sessions (out of 4)	2: 5 3: 1 4: 94	2: 4 3: 0 4: 96	2: 11 3: 0 4: 89	2: 20 3: 1 4: 279	$\chi(4) = 6.58$, $p = 0.16$	
FD, mm	0.08 ± 0.04	0.10 ± 0.05	0.13 ± 0.06	0.10 ± 0.06	$F(2,297) = 29.44$, $p < 0.01$**	Ov-Le: $p = 0.03$* Ob-Le: $p < 0.01$** Ob-Ob: $p < 0.01$**
Bilateral habenula volume, mm^3	44.95 ± 3.79	45.68 ± 3.10	45.11 ± 3.82	45.25 ± 3.59	$F(2,297) = 1.16$, $p = 0.32$	

First, all unrelated individuals with an obese BMI and HbA1c <5.7 were selected, and subsequently, subjects with lean and overweight BMI were matched on age, sex, ethnicity, SES, handedness, depression score, smoking status, and the number of resting-state scans available using optimal pair matching in R. Data are displayed as mean ± SD.

[a]ANOVA or chi-square performed to detect differences between groups.

*$p < 0.05$, **$p < 0.001$, ***$p < 0.0001$, significant difference between the group.

BMI, body mass index; FD, frame-wise displacement; HbA1c, hemoglobin A1c; rs-fMRI, resting-state functional magnetic resonance imaging; SD, standard deviation; SES, socioeconomic status.

TABLE 2. SUBJECT CHARACTERISTICS FOR EXPLORATORY HEMOGLOBIN A1C SAMPLE

	Healthy HbA1c (<5.7), n = *36*	*Prediabetic (HbA1c ≥5.7),* n = *36*	*All subjects,* n = *72*	*Statistics*	
				t/χ^a	*p*
Age, years	28.69 ± 3.73	28.83 ± 4.46	28.76 ± 4.08	−0.14	0.89
Sex, F/M	21 F/15 M	21 F/15 M	42 F/30 M	0.00	1.00
Ethnicity	Am. Indian: 0 Asian: 5 Black: 11 More than one: 1 Unknown: 1 White: 18	Am. Indian: 1 Asian: 5 Black: 11 More than one: 1 Unknown: 1 White: 17	Am. Indian: 1 Asian: 10 Black: 22 More than one: 2 Unknown: 2 White: 35	1.03	0.96
BMI, kg/m^2	26.96 ± 4.87	28.24 ± 5.53	27.60 ± 5.22	−1.05	0.29
BMI category	Lean: 15 Overweight: 11 Obese: 10	Lean: 12 Overweight: 11 Obese: 13	Lean: 27 Overweight: 22 Obese: 23	0.72	0.69
SES	18.89 ± 5.52	18.25 ± 6.06	18.57 ± 5.76	0.47	0.64
Blood pressure					
Systolic, mmHg	126.40 ± 13.51	127.40 ± 14.07	126.90 ± 13.71	−0.32	0.75
Diastolic, mmHg	78.19 ± 9.54	78.86 ± 11.26	78.53 ± 10.36	−0.27	0.79
HbA1c, %	5.17 ± 0.34	5.79 ± 1.31	5.48 ± 4.05	−10.33	<0.01**
Handedness	71.67 ± 36.17	62.22 ± 5.11	66.94 ± 4.42	0.91	0.37
Depression score	47.56 ± 6.99	46.77 ± 7.65	47.17 ± 7.29	0.45	0.65
Smoking, yes/no	32 no/4 yes	31 no/5 yes	63 no/9 yes	0	1
FD	0.10 ± 0.04	0.11 ± 0.06	0.11 ± 0.05	−1.13	0.26
Bilateral habenula volume, mm^3	46.13 ± 3.63	45.53 ± 3.44	45.83 ± 3.52	0.72	0.47

First, all unrelated individuals with an HbA1c ≥5.7 were selected, and healthy HbA1c subjects were matched on BMI, age, sex, ethnicity, SES, handedness, depression score, and smoking status using optimal pair matching in RStudio. Data are displayed as mean ± SD.

[a]Student's *t*-test or chi-square performed to detect differences between groups.

**$p < 0.001$, significant difference between the groups.

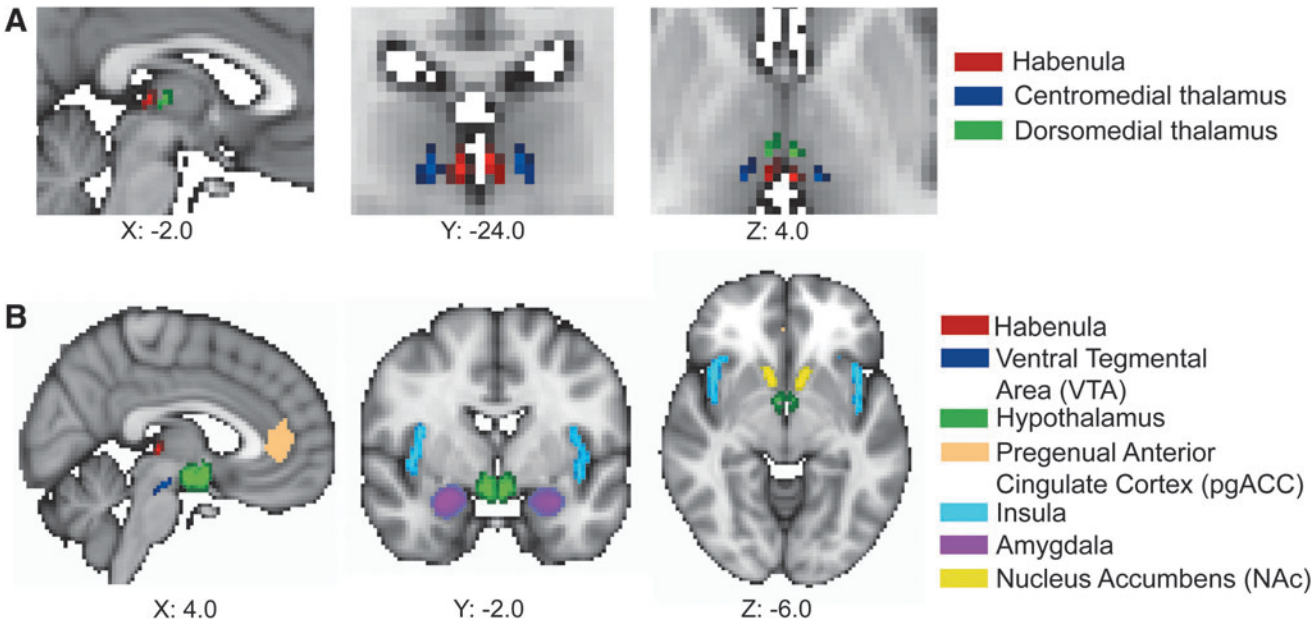

FIG. 1. Habenula and thalamic control seeds and target ROIs used in the analysis. **(A)** Mean map of habenula seeds and thalamic control seeds. **(B)** Target ROIs as used in the analysis (BMI sample), pgACC is a binary mask, while all other ROIs are probabilistic. The hypothalamus seed is an example of the subject-specific ROI, the habenula is the mean map of all subjects. Other ROIs are not subject-specific. BMI, body mass index; pgACC, pregenual anterior cingulate cortex; ROI, region of interest.

autocorrelation correction (Woolrich et al., 2001). The main model regressors were obtained by convolving predictors with a double gamma canonical hemodynamic response function; for details, see the study by Barch et al. (2013). The workbench command was used to extract the *Z*-values for subject-specific bilateral habenula seeds and used in second-level analyses.

Statistical analysis

Demographics were compared using analysis of variance (ANOVA; or *t*-test) for continuous variables and chi-square test for categorical variables in RStudio (2022, version 02.3). When ANOVA indicated between-group differences, Tukey's *post hoc* tests were used to determine which groups were different. To explore whole-brain FC of the habenula in the entire sample, a voxel-based analysis was performed using FSL Randomise with threshold free cluster enhancement (TFCE) correction and 5000 permutations (Smith and Nichols, 2009). For between-subject analysis of the effect of BMI on unique habenula rsFC, a linear model was used in RStudio (version 4.2.1, lme4 and lmerTest package). For the BMI sample, BMI was used as independent continuous variable, and age, sex, and HbA1c as covariates.

For the HbA1c sample, a similar model was used, but with an interaction term for BMI × HbA1c added. For the tfMRI data, the same linear models were used, only with habenula activity during the different contrasts as a dependent variable instead of rsFC. In our analyses, we opted for using BMI as a continuous variable, rather than categorical, since BMI is a continuous measure, and forcing continuous data into discrete categories can introduce arbitrariness and loss of information. The BMI cutoffs are based on population averages, thereby categorizing may oversimplify and misrepresent individual variation. For each model, FD was added to see if it would improve the model, which was not the case for any of the models. All data are displayed as mean ± standard error of the mean; a *p*-value <0.05 was considered statistically significant.

Results

Participants

Subject demographics for the BMI sample are shown in Table 1. Between the BMI categories (lean/overweight/obese), there was no significant difference in bilateral habenula volume. BMI, blood pressure, HbA1c, and FD were significantly different between the BMI categories. Tukey's *post hoc* analysis showed that both systolic and diastolic blood pressure were higher in individuals being overweight and obese compared with lean (all $p<0.01$), but not in those being obese compared with overweight (systolic $p=0.06$, diastolic $p=0.17$). HbA1c was only significantly different between individuals who were lean and obese ($p=0.03$), and FD was higher in the higher BMI categories (all *post hoc* tests $p<0.01$). For the exploratory HbA1c sample, subject demographics are displayed in Table 2. Between the subjects with a healthy HbA1c and those with prediabetes, we observed no significant differences in any of the parameters, except HbA1c.

Bilateral habenula rsFC in the whole brain

In the BMI sample ($n=300$), the habenula showed a widespread pattern of connectivity (Fig. 2), including connections to thalamus, VTA, cingulate cortex (anterior, posterior), paracingulate, insula, caudate, (pre)cuneus, and several parietal and occipital cortical areas (all $p_{\text{TFCE-corrected}}<0.01$ and $t>8$). No areas with negative rsFC were found (using $p_{\text{TFCE-corrected}}<0.01$ as threshold). In the HbA1c sample, a similar pattern was observed, although less widespread, but including thalamus, VTA, cingulate cortex (anterior, posterior), paracingulate, and caudate (Supplementary Fig. S1).

Associations between BMI and habenula rsFC

The ROI-to-ROI analysis showed no association between FC of the habenula with reward-related areas and BMI (Table 3; VTA: $t=0.52$, $p_{\text{FDR}}=0.96$; hypothalamus: $t=-0.19$, $p_{\text{FDR}}=0.96$; pgACC: $t=0.05$, $p_{\text{FDR}}=0.96$; amygdala: $t=0.07$, $p_{\text{FDR}}=0.96$; insula: $t=-0.83$, $p_{\text{FDR}}=0.96$; NAc: $t=1.13$, $p_{\text{FDR}}=0.96$).

Exploratory associations between BMI and HbA1c and habenula rsFC

In the secondary, exploratory, HbA1c sample, we found a significant BMI × HbA1c interaction effect for the habenula-VTA connection ($t=-2.29$, $p=0.03$), although this did not survive correction for multiple comparisons ($p_{\text{FDR}}=0.15$; Table 4). The analysis revealed that the at lower HbA1c levels, habenula-VTA rsFC showed a more positive correlation with BMI, whereas at higher HbA1c values, FC showed a more negative correlation with BMI. For all other ROIs, no significant BMI × HbA1c interaction effects were found, that is, habenula-hypothalamus rsFC ($t=0.34$, $p=0.74$), habenula-pgACC ($t=-0.20$, $p=0.84$), habenula-insula ($t=1.13$, $p=0.26$), habenula-amygdala ($t=-0.56$, $p=0.58$), and habenula-NAc ($t=-0.67$, $p=0.50$).

Habenula activity during punishment and reward in gambling task

For the BMI sample, habenula activity was higher during punishment than reward trials (Fig. 3A; paired *t*-test $t=2.18$, $df=296$, $p=0.03$*). Habenula activity during the ''punishment>reward'' contrast did not correlate with BMI, as measured with a linear model ($t=1.28$, $p=0.20$; Table 5). In the exploratory HbA1c sample, habenula activity was not different between punishment and reward (Fig. 3B; paired *t*-test $t=0.04$, $df=71$, $p=0.97$, effect size [Cohen's d] $=0.004$). No interaction effect of BMI × HbA1c was found for habenula activity during punishment>reward ($t=-1.94$, $p=0.06$), although the main effect of HbA1c was significant in the model including the interaction term ($t=2.05$, $p=0.04$*; Table 5).

Discussion

In this study, we investigated the association between BMI and habenula FC, as well as between BMI and habenula activity during a gambling task, by combining rs-fMRI and tfMRI data from a large high-quality data set from the HCP. In contrast to our hypothesis, we did not observe evidence for a relationship between BMI and habenula rsFC with reward-related regions, or between BMI and habenula activity during punishment in a gambling task. We also performed an exploratory analysis including HbA1c levels, which are a long-term blood glucose measure, and observed

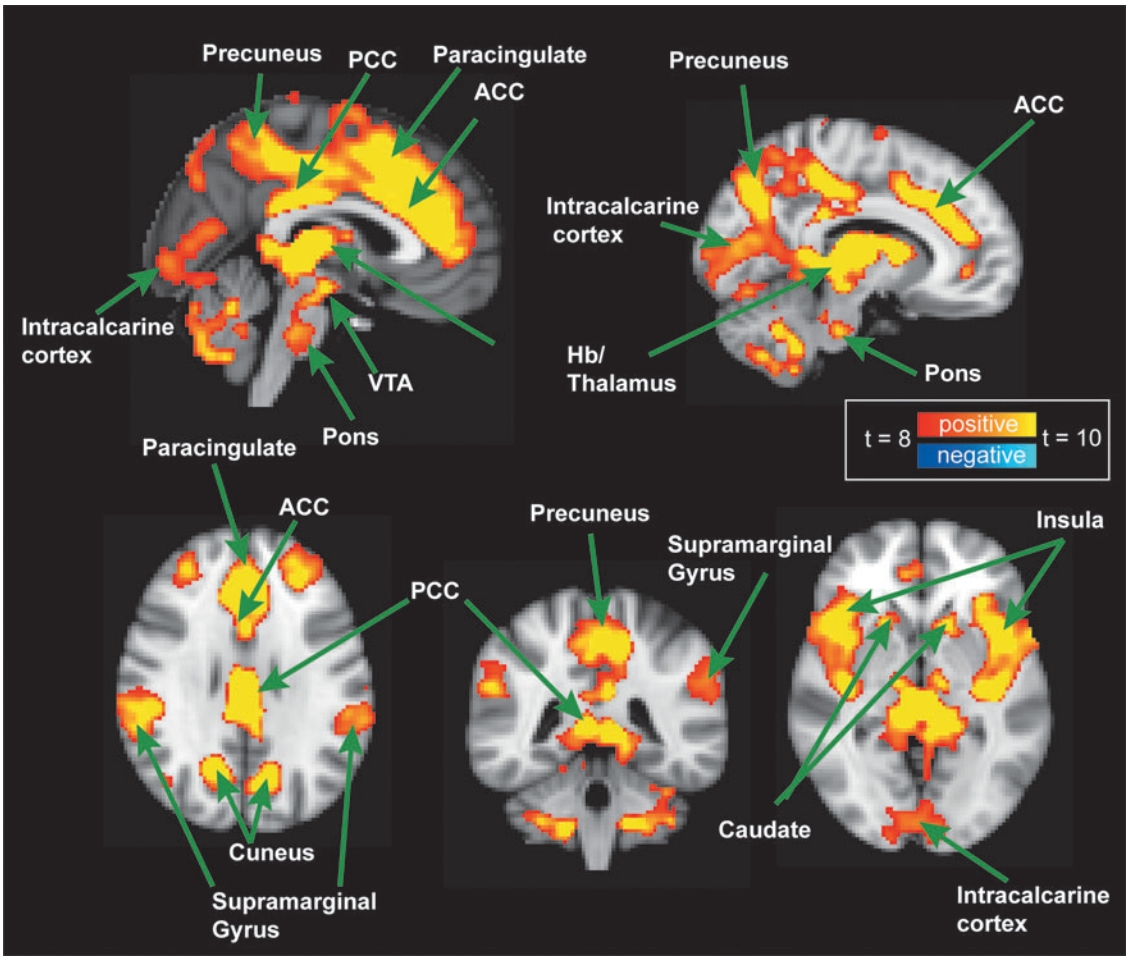

FIG. 2. Areas with significant bilateral habenula rsFC in the entire BMI sample ($n = 300$). t-Values of significant voxels ($p < 0.01$ and $t > 8$) are shown. ACC, anterior cingulate cortex; Hb, habenula; PCC, posterior cingulate cortex; rsFC, resting-state functional connectivity; VTA, ventral tegmental area.

a BMI × HbA1c interaction effect for habenula-VTA rsFC. However, this finding did not survive correction for multiple comparisons, and thus, additional studies are warranted to investigate this preliminary observation in more detail.

Our hypothesis that BMI would correlate with habenula rsFC is based on the previous literature indicating that weight loss is associated with changes in functional and structural rsFC between the habenula and homeostatic and reward-related regions (Maldonado et al., 2018; Wang et al., 2023; Wang et al., 2022). Historically, the habenula is regarded as the anti-reward nucleus, with increased firing upon aversive stimuli or omission of expected rewards, thus signaling a reward prediction error (Matsumoto and Hikosaka, 2007). It receives and sends many afferent and efferent connections throughout the brain, as indicated by the extensive rsFC in the whole brain analysis observed by us and others (Ely et al., 2016). This connectivity includes dopaminergic, serotonergic, and norepinephrine systems, which enables the habenula to integrate reward status and signal salience to optimize behavioral output.

We found no correlations between BMI and rsFC of the habenula and multiple ROIs, including the VTA, NAc, insula, pgACC, amygdala, and hypothalamus. In contrast, others have reported changes in local FC density within the habenula in obesity (Wang et al., 2023; Wang et al., 2022). In addition, several human fMRI studies report alterations in structural or FC with the habenula following weight loss (Maldonado et al., 2018; Wang et al., 2023; Wang et al., 2022). The different findings in our study and the weight loss studies are likely explained by differences in study design.

First, Wang et al. (2023, 2022) performed within-subject comparisons, whereas we performed between-subject correlations in this study. Second, Wang et al. (2023, 2022) analyzed local FC density, a relatively novel metric, whereas we used correlation strength as a connectivity metric. Finally, Maldonado et al. (2018) investigated the rsFC between the habenula and the NAc and hypothalamus and reported reduced rsFC in both connections in patients with cancer-associated weight loss. The ROIs that we included in our analysis were not analyzed by Wang et al. (2023, 2022). It is important to note that (cancer-associated) weight loss is a distinct phenomenon from obesity and involves metabolic changes beyond just a reduction in body weight.

In line with the literature reporting that the habenula is activated upon punishment (Matsumoto and Hikosaka, 2007),

Table 3. Statistical Output from Linear Model on Body Mass Index Relationship

	Coefficients					
ROI	*Name*	*Estimates*	*t*	$p_{uncorrected}$	p_{FDR}	*Model statistics*
VTA	BMI	0.00015	0.52	0.61	0.96	$F(4,289) = 0.78$, $p = 0.54$
	HbA1c	−0.00039	0.07	0.94	0.94	
	Sex	−0.00444	−1.61	0.11	0.28	
	Age	0.00007	0.18	0.86	0.86	
Hypothalamus	BMI	−0.00002	−0.19	0.85	0.96	$F(4,289) = 0.72$, $p = 0.58$
	HbA1c	0.00285	1.45	0.15	0.44	
	Sex	0.00004	0.04	0.97	0.97	
	Age	−0.00012	−0.87	0.38	0.67	
pgACC	BMI	0.00001	0.05	0.96	0.96	$F(4,289) = 1.12$, $p = 0.35$
	HbA1c	−0.00149	−0.64	0.52	0.78	
	Sex	−0.00177	−1.49	0.14	0.28	
	Age	−0.00027	−1.62	0.11	0.64	
Insula	BMI	−0.00006	−0.83	0.41	0.96	$F(4,289) = 1.26$, $p = 0.29$
	HbA1c	−0.00029	−0.22	0.83	0.94	
	Sex	0.00113	1.66	0.10	0.28	
	Age	−0.00007	−0.76	0.45	0.67	
Amygdala	BMI	0.00001	0.07	0.94	0.96	$F(4,289) = 0.75$, $p = 0.56$
	HbA1c	−0.00281	−1.57	0.40	0.44	
	Sex	0.00010	0.11	0.33	0.97	
	Age	−0.00029	−0.58	0.26	0.67	
NAc	BMI	0.00022	1.13	0.26	0.96	$F(4,289) = 1.07$, $p = 0.37$
	HbA1c	−0.00309	−0.84	0.40	0.78	
	Sex	0.00185	0.98	0.33	0.49	

FC as dependent variable, BMI as independent, HbA1c, sex, and age as covariates. *p*-Values are corrected for multiple comparisons using the FDR method. With a significance level of $p = 0.05$, no significance was found for any of the models or the coefficients.

FDR, false discovery rate; NAc, nucleus accumbens; pgACC, pregenual anterior cingulate cortex; VTA, ventral tegmental area.

our study found an increase in habenula activity during punishment compared with reward. However, we could not replicate this observation in the smaller HbA1c sample. We hypothesized that habenula activity would correlate with BMI because learning from prediction errors, which is encoded by the habenula, is disrupted in obesity (Mathar et al., 2017). However, the HCP gambling task does not include an anticipatory phase, which limits the formation of predictions, and therefore, our hypothesis could not be tested as such. Although reward sensitivity is positively associated with eating behavior, such as binge eating and the consumption of palatable foods (Davis et al., 2007; Franken and Muris, 2005; Tetley et al., 2010), the relationship between reward sensitivity and BMI is less clear (Sutton et al., 2022). This likely explains why we did not observe a correlation between habenula activity upon punishment and BMI.

BMI alone might not be an accurate indicator of metabolic health. To assess this, we also investigated the role of HbA1c levels, which reflect long-term blood glucose levels, in addition to BMI. This is particularly important as HbA1c levels are the only measurement of (recent) metabolic health registered in the HCP data set, as no information on food intake, weight development, satiety status, or blood glucose levels at the time of scanning is available. The habenula might play a role in glucose metabolism, as lesioning the habenula increased insulin sensitivity in a rat model for diabetes mellitus type 2 (DM2) (Qu et al., 2020).

Furthermore, habenular TCFL2, a protein involved in the GLP-1 signaling cascade, regulates blood glucose levels in response to nicotine in rodents (Duncan et al., 2019). These observations might be translatable to humans as a positive correlation between habenula volume and HbA1c levels has been observed in nicotine smokers (Jha et al., 2021). Therefore, we hypothesized glucose- and BMI-dependent changes in habenula rsFC, which we observed for the habenula-VTA connection; in obese individuals, a positive relationship between HbA1c level and rsFC was observed. However, this finding did not survive correction for multiple comparisons, indicating that future research is needed to assess the implication of this exploratory finding.

Open-access data sets such as HCP provide high-quality data with large sample sizes. However, despite using a relatively large sample ($n = 300$), which should be sufficient to report (clinically) relevant associations using rsFC (Gratton et al., 2022; Marek et al., 2022), we did not find any correlations with BMI. Despite the high quality and high resolution that HCP offers, it does not provide exhaustive information about the metabolic status of the included subjects. For example, fasting status at the time of scanning is not registered. This is unfortunate, as is has been shown that the satiation status of an individual can influence BOLD response during fMRI and that ingestion of different nutrients can also affect BOLD responses (Al-Zubaidi et al., 2019; Roelofs et al., 2022; Thomas et al., 2015; Van Opstal et al., 2019; Zhang et al., 2015).

Moreover, patterns of recent weight loss or gain were also not registered, which can also alter the neural circuits associated with reward-related responses (Murdaugh et al., 2012; Zeighami et al., 2021; Zhang et al., 2016). Therefore, such open-access data sets are particularly valuable in conjunction with smaller experimental studies with extensive characterization

Table 4. Linear Model with Body Mass Index × Hemoglobin A1c Interaction Effect for Each Region of Interest

	Coefficients					
ROI	*Name*	*Estimates*	*t*	$p_{uncorrected}$	p_{FDR}	*Model statistics*
VTA	BM:HbA1c	−0.00228	−2.29	0.03*	0.15	$F(5,65) = 1.35$, $p = 0.25$
	BMI	0.01298	2.36	0.02*	0.13	
	HbA1c	0.06229	2.30	0.02*	0.13	
	Sex	−0.00417	−0.93	0.35	0.63	
	Age	−0.00009	−0.17	0.86	0.97	
Hypothalamus	BMI:HbA1c	0.00013	0.34	0.74	0.84	$F(5,65) = 0.35$, $p = 0.88$
	BMI	−0.00073	−0.35	0.73	0.80	
	HbA1c	−0.00503	−0.48	0.63	0.82	
	Sex	−0.00162	−0.95	0.35	0.63	
	Age	−0.00008	−0.40	0.86	0.97	
pgACC	BMI:HbA1c	−0.00006	−0.20	0.84	0.84	$F(5,65) = 0.41$, $p = 0.84$
	BMI	0.00042	0.25	0.80	0.80	
	HbA1c	0.00188	0.23	0.82	0.82	
	Sex	−0.00156	−1.14	0.26	0.63	
	Age	−0.00012	−0.72	0.48	0.97	
Insula	BMI:HbA1c	0.00036	1.13	0.26	0.79	$F(5,65) = 0.41$, $p = 0.84$
	BMI	−0.00212	−1.19	0.24	0.72	
	HbA1c	−0.00904	−1.03	0.31	0.82	
	Sex	0.00040	0.28	0.78	0.94	
	Age	0.00032	−0.04	0.97	0.97	
Amygdala	BMI:HbA1c	−0.00023	−0.56	0.58	0.84	$F(5,65) = 0.84$, $p = 0.53$
	BMI	0.00146	0.63	0.53	0.80	
	HbA1c	0.00316	0.28	0.78	0.82	
	Sex	0.00007	0.04	0.97	0.97	
	Age	0.00032	1.41	0.16	0.97	
NAc	BMI:HbA1c	−0.00067	−0.67	0.50	0.84	$F(5,65) = 0.40$, $p = 0.85$
	BMI	0.00348	0.63	0.53	0.80	
	HbA1c	0.01487	0.55	0.58	0.82	
	Sex	−0.00361	−0.81	0.42	0.63	
	Age	−0.00035	−0.65	0.52	0.97	

Using a linear model with age, sex, and HbA1c as covariates, the habenula-VTA connection showed a significant BMI × HbA1c interaction effect; however, it did not survive multiple comparison correction ($n = 72$).

*$p < 0.05$.

ROI, region of interest.

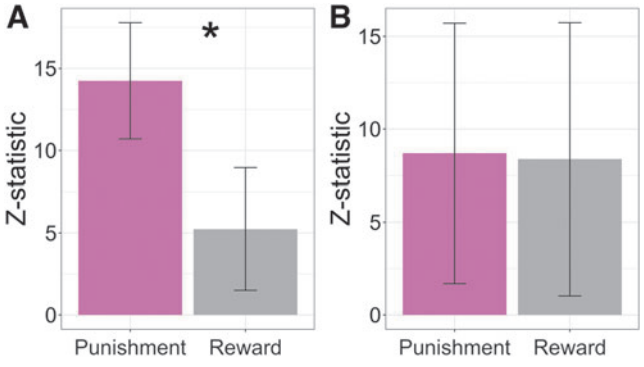

FIG. 3. Habenula activity during gambling task for both data sets. **(A)** In the BMI sample ($n = 300$), average habenula activity (BOLD) during punishment (left) is significantly higher than during reward (right). **(B)** In the HbA1c sample, habenula activity is not different between punishment and reward. All data mean ± SEM, $p < 0.05$ was considered significant. *$p < 0.05$. BOLD, blood oxygen level dependent; SEM, standard error of the mean.

of metabolic health. In addition, smoking is a possible confounder, as it is a risk factor for DM2, and habenula volume correlates with HbA1c in nicotine-smoking individuals (Jha et al., 2021). The number of smokers in the HbA1c sample is very small, limiting our ability for conclusions. Finally, future studies might want to focus on distinguishing the medial and lateral habenula, as both nuclei have different connections and functions, using 7T fMRI, which is already possible in structural MRI scans (Strotmann et al., 2014).

In conclusion, we did not find evidence for an association between BMI and habenula FC or its activity during punishment using an ROI-to-ROI analysis on high-quality data from HCP. An additional, exploratory, analysis suggested that habenula-VTA rsFC positively correlates with blood HbA1c levels in individuals with obesity. Future studies should take into consideration different metabolic states of participants (e.g., fasted/fed) or work with fMRI tasks that also include an anticipatory phase to adequately study reward prediction error. While we did not observe clear associations between habenula rsFC and reward-related activity and BMI, studying the habenula and its potential role in metabolic health remains important in light of the current obesity epidemic.

Table 5. Statistical Output from Linear Model on Habenula Activity During Gambling Task for Both Data Sets

	Coefficients				
Punishment>reward Bilateral habenula	*Name*	*Estimate*	*t*	*p*	*Model statistics*
BMI sample ($n=300$)	BMI	1.10	1.28	0.20	$F(4,292)=1.05$, $p=0.40$
	HbA1c	3.25	0.20	0.84	
	BMI × HbA1c	N/A	N/A	N/A	
HbA1c sample ($n=72$)	BMI	37.39	1.81	0.07	$F(5,66)=1.34$, $p=0.26$
	HbA1c	209.38	2.05	0.04*	
	BMI × HbA1c	−7.22	−1.94	0.06	

Model with activity as dependent variable, and BMI and HbA1c as independent for the BMI sample ($n=300$), and BMI × HbA1c for the HbA1c sample ($n=72$). Age and sex were included as covariates in both models.

Acknowledgments

We would like to thank the Human Connectome Project for making these data available. Furthermore, we would like to thank Dr. Joo-Won Kim (Baylor College of Medicine, Houston, Texas) for the publicly available habenula segmentation algorithm and assisting with implementation, as well as Dr. Benjamin Billot (Massachusetts Institute of Technology) for the publicly available hypothalamus segmentation and aiding in the implementation.

Data Availability

Scripts and algorithms used in this study are publically available at margo-tje/fMRI_HCP_Habenula:Scripts used in''InvestigatingHabenulaFunctionalConnectivityandReward-RelatedActivityinObesityusingHumanConnectomeProjectData'' (github.com).

Authors' Contributions

M.S.: Conceptualization, methodology, software, formal analysis, visualization, methodology, writing—original draft. I.G.S.d.L.: Methodology, software, formal analysis, writing—review and editing. J.D.M.: Conceptualization, writing—review and editing, supervision. A.S.: Conceptualization, methodology, resources, writing—review and editing, supervision. S.E.l.F.: Conceptualization, writing—review and editing, supervision.

Author Disclosure Statement

No competing financial interests exist.

Funding Information

This work was supported by an AMC PhD fellowship grant awarded by the AMC Executive Board.

Supplementary Material

Supplementary Figure S1

References

Afshin A, Forouzanfar M, Reitsma M, et al. Health effects of overweight and obesity in 195 countries over 25years. N Engl J Med 2017;377(1):13–27.

Al-Zubaidi A, Heldmann M, Mertins A, et al. Impact of hunger, satiety, and oral glucose on the association between insulin and resting-state human brain activity. Front Hum Neurosci 2019;13:162.

Avery JA, Powell JN, Breslin FJ, et al. Obesity is associated with altered mid-insula functional connectivity to limbic regions underlying appetitive responses to foods. J Psychopharmacol 2017;31(11):1475–1484.

Barch DM, Burgess GC, Harms MP, et al. Function in the human connectome: Task-fMRI and individual differences in behavior. Neuroimage 2013;80:169–189.

Behzadi Y, Restom K, Liau J, et al. A component based noise correction method (CompCor) for BOLD and perfusion based fMRI. Neuroimage 2007;37(1):90–101.

Berridge KC. 'Liking' and 'wanting' food rewards: Brain substrates and roles in eating disorders. Physiol Behav 2009; 97(5):537–550.

Berthoud H-R. Metabolic and hedonic drives in the neural control of appetite: Who is the boss? Curr Opin Neurobiol 2011; 21(6):888–896.

Berthoud H-R, Morrison C. The brain, appetite, and obesity. Annu Rev Psychol 2008;59:55–92.

Billot B, Bocchetta M, Todd E, et al. Automated segmentation of the hypothalamus and associated subunits in brain MRI. Neuroimage 2020;223:117287.

Bonadonna R, De Fronzo R. Glucose metabolism in obesity and type 2 diabetes. Diabete Metab 1991;17(1 Pt 2):112–135.

Collins DL, Holmes CJ, Peters TM, et al. Automatic 3-D model-based neuroanatomical segmentation. Hum Brain Mapp 1995;3(3):190–208.

Davis C, Curtis C, Tweed S, et al. Psychological factors associated with ratings of portion size: relevance to the risk profile for obesity. Eat Behav 2007;8(2):170–176.

Desikan RS, Ségonne F, Fischl B, et al. An automated labeling system for subdividing the human cerebral cortex on MRI scans into gyral based regions of interest. Neuroimage 2006;31(3):968–980.

Doucet GE, Rasgon N, McEwen BS, et al. Elevated body mass index is associated with increased integration and reduced cohesion of sensory-driven and internally guided resting-state functional brain networks. Cereb Cortex 2017;28(3):988–997.

Duncan A, Heyer MP, Ishikawa M, et al. Habenular TCF7L2 links nicotine addiction to diabetes. Nature 2019; 574(7778):372–377.

Eckel RH, Grundy SM, Zimmet PZ. The metabolic syndrome. Lancet 2005;365(9468):1415–1428.

Ely BA, Xu J, Goodman WK, et al. Resting-state functional connectivity of the human habenula in healthy individuals: Associations with subclinical depression. Hum Brain Mapp 2016; 37(7):2369–2384.

Forbes EE, Hariri AR, Martin SL, et al. Altered striatal activation predicting real-world positive affect in adolescent major depressive disorder. Am J Psychiatry 2009;166(1): 64–73.

Franken IH, Muris P. Individual differences in reward sensitivity are related to food craving and relative body weight in healthy women. Appetite 2005;45(2):198–201.

García-García I, Jurado MÁ, Garolera M, et al. Alterations of the salience network in obesity: A resting-state fMRI study. Hum Brain Mapp 2013;34(11):2786–2797.

Gershon RC, Wagster MV, Hendrie HC, et al. NIH toolbox for assessment of neurological and behavioral function. Neurology 2013;80(11 Suppl 3):S2–S6.

Glasser MF, Sotiropoulos SN, Wilson JA, et al. The minimal preprocessing pipelines for the Human Connectome Project. Neuroimage 2013;80:105–124.

Gratton C, Nelson SM, Gordon EM. Brain-behavior correlations: Two paths toward reliability. Neuron 2022;110(9): 1446–1449.

Gunstad J, Paul RH, Cohen RA, et al. Relationship between body mass index and brain volume in healthy adults. Int J Neurosci 2008;118(11):1582–1593.

Herrmann MJ, Tesar AK, Beier J, et al. Grey matter alterations in obesity: A meta-analysis of whole-brain studies. Obes Rev 2019;20(3):464–471.

Jallut D, Golay A, Munger R, et al. Impaired glucose tolerance and diabetes in obesity: a 6-year follow-up study of glucose metabolism. Metabolism 1990;39(10):1068–1075.

Jha MK, Kim J-w, Kenny PJ, et al. Smoking status links habenular volume to glycated hemoglobin: Findings from the Human Connectome Project-Young Adult. Psychoneuroendocrinology 2021;131:105321.

Ji H, Shepard PD. Lateral habenula stimulation inhibits rat midbrain dopamine neurons through a GABAA receptor-mediated mechanism. J Neurosci 2007;27(26):6923–6930.

Kim J-W, Xu J. Automated human habenula segmentation from T1-weighted magnetic resonance images using V-Net. bioRxiv 2022:2022;2001.2025.477768.

Kullmann S, Heni M, Veit R, et al. The obese brain: association of body mass index and insulin sensitivity with resting state network functional connectivity. Hum Brain Mapp 2012; 33(5):1052–1061.

Lawson RP, Seymour B, Loh E, et al. The habenula encodes negative motivational value associated with primary punishment in humans. Proc Natl Acad Sci U S A 2014;111(32): 11858–11863.

Li G, Hu Y, Zhang W, et al. Resting activity of the hippocampus and amygdala in obese individuals predicts their response to food cues. Addict Biol 2020:26(3):e12974.

Maldonado M, Molfese DL, Viswanath H, et al. The habenula as a novel link between the homeostatic and hedonic pathways in cancer-associated weight loss: a pilot study. J Cachexia Sarcopenia Muscle 2018;9(3):497–504.

Marek S, Tervo-Clemmens B, Calabro FJ, et al. Reproducible brain-wide association studies require thousands of individuals. Nature 2022;603(7902):654–660.

Martin-Rodriguez E, Guillen-Grima F, Martí A, et al. Comorbidity associated with obesity in a large population: The APNA study. Obes Res Clin Pract 2015;9(5):435–447.

Mathar D, Neumann J, Villringer A, et al. Failing to learn from negative prediction errors: Obesity is associated with alterations in a fundamental neural learning mechanism. Cortex 2017;95:222–237.

Matsumoto M, Hikosaka O. Lateral habenula as a source of negative reward signals in dopamine neurons. Nature 2007; 447(7148):1111.

Murdaugh DL, Cox JE, Cook EW 3rd, et al. fMRI reactivity to high-calorie food pictures predicts short-and long-term outcome in a weight-loss program. Neuroimage 2012;59(3): 2709–2721.

Oldfield RC. The assessment and analysis of handedness: The Edinburgh inventory. Neuropsychologia 1971;9(1):97–113.

Omelchenko N, Bell R, Sesack SR. Lateral habenula projections to dopamine and GABA neurons in the rat ventral tegmental area. Eur J Neurosci 2009;30(7):1239–1250.

Pauli WM, Nili AN, Tyszka JM. A high-resolution probabilistic in vivo atlas of human subcortical brain nuclei. Sci Data 2018;5(1):180063.

Qu P, Wang Y, Liu L, et al. Habenula lesions improve glucose metabolism in rats with type 2 diabetes by increasing insulin sensitivity and inhibiting gluconeogenesis. BMJ Open Diabetes Res Care 2020;8(1):e001250.

Roelofs TJ, Straathof M, van der Toorn A, et al. Diet as connecting factor: Functional brain connectivity in relation to food intake and sucrose tasting, assessed with resting-state functional MRI in rats. J Neurosci Res 2022;100(5):1182–1190.

Sadler JR, Shearrer GE, Burger KS. Alterations in ventral attention network connectivity in individuals with prediabetes. Nutr Neurosci 2021;24(2):140–147.

Schaefer A, Kong R, Gordon EM, et al. Local-global parcellation of the human cerebral cortex from intrinsic functional connectivity MRI. Cereb Cortex 2018;28(9):3095–3114.

Scharmüller W, Übel S, Ebner F, et al. Appetite regulation during food cue exposure: A comparison of normal-weight and obese women. Neurosci Lett 2012;518(2):106–110.

Smith SM, Beckmann CF, Andersson J, et al. Resting-state fMRI in the human connectome project. Neuroimage 2013;80:144–168.

Smith SM, Nichols TE. Threshold-free cluster enhancement: Addressing problems of smoothing, threshold dependence and localisation in cluster inference. Neuroimage 2009; 44(1):83–98.

Stamatakis AM, Van Swieten M, Basiri ML, et al. Lateral hypothalamic area glutamatergic neurons and their projections to the lateral habenula regulate feeding and reward. J Neurosci 2016;36(2):302–311.

Stice E, Figlewicz DP, Gosnell BA, et al. The contribution of brain reward circuits to the obesity epidemic. Neurosci Biobehav Rev 2013;37(9):2047–2058.

Stice E, Spoor S, Bohon C, et al. Relation between obesity and blunted striatal response to food is moderated by TaqIA A1 allele. Science 2008;322(5900):449–452.

Stoeckel LE, Kim J, Weller RE, et al. Effective connectivity of a reward network in obese women. Brain Res Bull 2009;79(6): 388–395.

Strotmann B, Heidemann RM, Anwander A, et al. High-resolution MRI and diffusion-weighted imaging of the human habenula at 7 tesla. J Magn Reson Imaging 2014;39(4):1018–1026.

Sutton CA, L'Insalata AM, Fazzino TL. Reward sensitivity, eating behavior, and obesity-related outcomes: A systematic review. Physiol Behav 2022:252;113843.

Tetley AC, Brunstrom JM, Griffiths PL. The role of sensitivity to reward and impulsivity in food-cue reactivity. Eat Behav 2010;11(3):138–143.

Thomas JM, Higgs S, Dourish CT, et al. Satiation attenuates BOLD activity in brain regions involved in reward and

increases activity in dorsolateral prefrontal cortex: An fMRI study in healthy volunteers. Am J Clin Nutr 2015; 101(4):697–704.

Uğurbil K, Xu J, Auerbach EJ, et al. Pushing spatial and temporal resolution for functional and diffusion MRI in the Human Connectome Project. Neuroimage 2013;80:80–104.

Van Essen DC, Smith SM, Barch DM, et al. The WU-Minn human connectome project: An overview. Neuroimage 2013;80:62–79.

Van Opstal A, Kaal I, Van den Berg-Huysmans A, et al. Dietary sugars and non-caloric sweeteners elicit different homeostatic and hedonic responses in the brain. Nutrition 2019;60:80–86.

Wang G-J, Shokri Kojori E, Yuan K, et al. Inhibition of food craving is a metabolically active process in the brain in obese men. Int J Obes 2020;44(3):590–600.

Wang J, Ji G, Li G, et al. Habenular connectivity predict weight loss and negative emotional-related eating behavior after laparoscopic sleeve gastrectomy. Cereb Cortex 2023;33(5): 2037–2047.

Wang J, Li G, Hu Y, et al. Habenular and mediodorsal thalamic connectivity predict persistent weight loss after laparoscopic sleeve gastrectomy. Obesity (Silver Spring) 2022;30(1):172–182.

Wani RT. Socioeconomic status scales-modified Kuppuswamy and Udai Pareekh's scale updated for 2019. J Fam Med Prim Care 2019;8(6):1846.

Waterson MJ, Horvath TL. Neuronal regulation of energy homeostasis: beyond the hypothalamus and feeding. Cell Metab 2015;22(6):962–970.

Whitfield-Gabrieli S, Nieto-Castanon A. Conn: A functional connectivity toolbox for correlated and anticorrelated brain networks. Brain Connect 2012;2(3):125–141.

Woolrich MW, Ripley BD, Brady M, et al. Temporal autocorrelation in univariate linear modeling of FMRI data. Neuroimage 2001;14(6):1370–1386.

WU-Minn HCP. 1200 Subjects Data Release Reference Manual. 2017. Available from: https://www.humanconnectome.org [Last accessed: July 23, 2019].

Yang L-M, Hu B, Xia Y-H, et al. Lateral habenula lesions improve the behavioral response in depressed rats via increasing the serotonin level in dorsal raphe nucleus. Behav Brain Res 2008;188(1):84–90.

Zeighami Y, Iceta S, Dadar M, et al. Spontaneous neural activity changes after bariatric surgery: A resting-state fMRI study. Neuroimage 2021;241:118419.

Zhang B, Tian D, Yu C, et al. Altered baseline brain activities before food intake in obese men: A resting state fMRI study. Neurosci Lett 2015;584:156–161.

Zhang Y, Ji G, Xu M, et al. Recovery of brain structural abnormalities in morbidly obese patients after bariatric surgery. Int J Obes 2016;40(10):1558–1565.

Address correspondence to:
Susanne E. la Fleur
Endocrine Laboratory
Department of Laboratory Medicine
Amsterdam UMC
Location University of Amsterdam
Meibergdreef 9
Amsterdam 1105 AZ
The Netherlands

E-mail: s.e.lafleur@amsterdamumc.nl